THE POSITION RESOLUTION OF THE TIME PROJECTION CHAMBER AT TRIUMF

C.K. Hargrove, H. Mes
National Research Council of Canada, Ottawa, Ont., Canada K1A 0R6

A. Bennett, D.A. Bryman*, M. Hasinoff†, J.A. Macdonald, J.M. Poutissou†, T. Numao*, J. Spuller
TRIUMF, Vancouver, B.C., Canada V6T 2A3

G. Azuelos, R. Poutissou
Université de Montréal, Montréal, P.Q., Canada H3C 3J7

M. Blecher, K. Gotow
Virginia Polytechnic Institute and State University, Blacksburg, VA, USA 24061

A.L. Carter
Carleton University, Ottawa, Ont., Canada K1S 5B6

Summary

We have investigated the spatial resolution of the TRIUMF time projection chamber (TPC). The dominant effects on the resolution are diffusion, track-anode crossing angle, $\vec{E}\times\vec{B}$ forces in the region of the anode wire and clustering of the primary ionization. A formulation of these effects has been used to determine the mean collision time, the diffusion constant, the Lorentz angle in the anode wire region and the spatial resolution as a function of the crossing angle for a gas mixture of Ar (80%), CH_4 (20%) at atmospheric pressure. The minimum resolution, $\sigma \sim 200\mu m$, occurs when the track crossing angle equals the Lorentz angle. As the angle moves away from this value the resolution deteriorates rapidly due to the discrete nature of the ionization process.

Introduction

An apparatus based on the principle of the time projection chamber (TPC)[1] has been developed to search for the lepton number violating nuclear muon capture reactions:

$$\mu^- Z \rightarrow e^- Z$$

$$\mu^- Z \rightarrow e^+ (Z-2)$$

The TPC is a large volume drift chamber with uniform parallel electric and magnetic fields. Several effects which influence the spatial resolution of the TPC have been studied. An important aspect of TPC operation is the reduction of transverse diffusion of the ionization electrons in the presence of parallel electric ($\vec{E}$) and magnetic ($\vec{B}$) fields ($\vec{E}\times\vec{B}=0$) in the drift region. In the neighbourhood of the endcap proportional wires there are necessarily regions where $\vec{E}\times\vec{B}\neq 0$ which significantly affect the shape of the drifting ionization cloud in a manner which depends on the angle at which the track crossed the wire. In addition, density fluctuations and clustering of the primary ionization deposited by a charged particle traversing the chamber gas are important considerations.

The TRIUMF TPC

The TRIUMF TPC[2,3] is shown in Fig. 1. Ionization tracks of charged particles which have traversed the chamber drift under the force of the electric field E=250 v/cm onto proportional wire modules in the endcaps. The gas used is a mixture of Ar(80%) and CH_4(20%) at atmospheric pressure and the magnetic field has a maximum operating value of B=9.5 kG. The drift velocity was measured to be U=7 cm/μsec. The endcap modules have 12 slots separated by 2.54 cm as shown in Fig. 2. A point charge on the anode would induce a charge distribution on the segmented cathode spreading over 2-3 pads each of width S=0.6 mm. By measuring the width of the cathode charge distribution the true anode charge distribution can be determined.

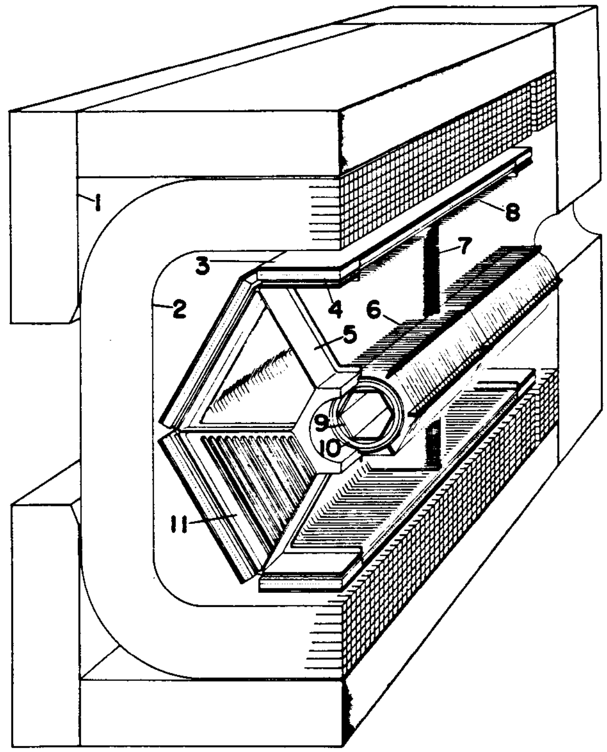

Fig. 1. A perspective view of the TPC. The numbered elements are: 1) the magnet iron, 2) the coil which has an inside field volume of 1.5m × 1.2m × 0.9m, 3) outer trigger scintillators, 4) outer trigger proportional counters, 5) endcap support frame, 6) central electric field cage wires, 7) central high voltage plane, 8) outer electric field cage wires, 9) inner trigger scintillators, 10) inner trigger cylindrical proportional wire chamber, 11) endcap proportional wire modules for track detection.

The cathode signal feeds a LRS TRA 510 amplifier and its output is digitized by the LRS 2280 12 bit ADC system. The amplifier pulse width at the base is 1.2 μsec. The noise of the system is ~2 fC and the wire gain is ~5×10^4. The sum of induced signals on the pads for minimum ionizing tracks is ~0.2 pC.

Data Analysis

The Pad Distributions

The distributions of charge on the cathode pads were fitted with a function f(x) chosen to minimize biases in the estimates of the centroids. Such biases were found to be as large as 200 μm for a simple Gaussian function. The function used was

*and University of Victoria
†and University of British Columbia

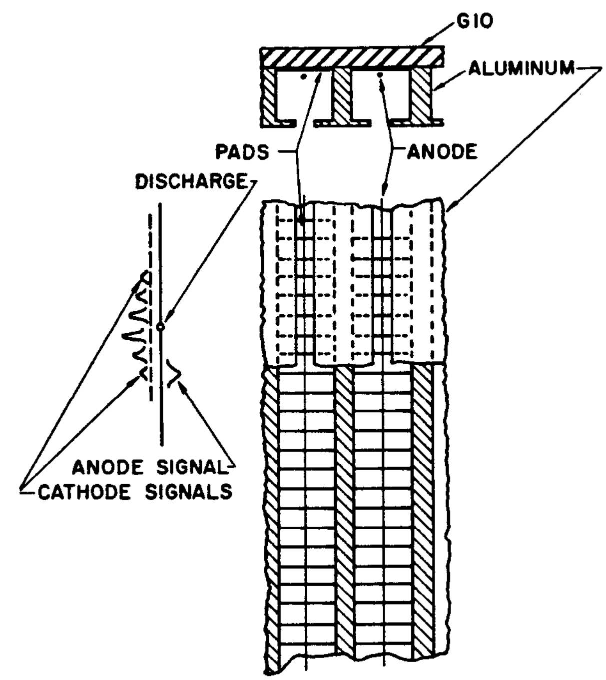

Fig. 2. Anode wire slots. The slots are machined out of a 19 mm thick plate. They are 19 mm wide and 17 mm deep. The remaining 2 mm has a 6.3 mm slot cut in it to allow the ionization access to the anode wires. The plate has a 6.3 mm G10 back plate which supports the anode wires in the slot and has the 6 mm wide cathode pads etched on it. The anode is 4 mm above the pads. The electrical connection to the pads is made by pins which go through the G10.

$$f(x) = \exp\left[p - \sqrt{w^2+m^2(x-x_o)^2}\right], \tag{1}$$

where: p is the amplitude parameter, w is the width parameter, x_o is the centre of the distribution and m is a constant. The full width at half maximum (FWHM) of this distribution is given by:

$$W = \frac{2S}{m}\sqrt{\ln 2(\ln 2+2w)} \ . \tag{2}$$

Three important effects contribute to the observed width W^* of the charge distribution induced on the cathode plane:

1. W_1 the intrinsic width of the measuring system
2. W_2 the width due to diffusion, and
3. W_3 the width due to the track-anode crossing angle and Lorentz forces.

The FWHM for a point source distribution is a constant W_1 = C1.

Diffusion

Diffusion plays an important role in spreading the charge distribution along the anode wire. The FWHM of diffusion normal to the drift direction in one dimension is:

$$W_2^o = 2.35\sqrt{\frac{2Dz}{U}} \tag{3}$$

where D is the diffusion constant, z the drift length and U the drift velocity. The diffusion constant is reduced in the presence of a magnetic field B according to the relation:

$$D(B) = D(0)/(1+\omega^2\tau^2) \ . \tag{4}$$

ω is the electron cyclotron frequency and τ is the mean electron collision time. This diffusion width normal to the track direction is projected onto the anode wire leading to:

$$W_2 = \frac{2.35}{\cos\theta}\sqrt{\frac{2D(0)z}{U(1+\omega^2\tau^2)}} \ . \tag{5}$$

The Angle Effect

In the absence of a magnetic field when the tracks are at an angle θ to the normal to the anode wire slot (Fig. 3a), the charge distribution at the anode wire is a square function with width H given by:

$$H = L\tan\theta \ . \tag{6}$$

Here L is the width of the slot. The observed cathode charge distribution is broader than that induced by a point source. The contribution to the FWHM of a square uniform distribution is:

$$W_3^o = \frac{2.35H}{2\sqrt{3}} \ . \tag{7}$$

E×B Effects in the Anode Slot

Effects of non-parallel electric ($\bar{E}$) and magnetic ($\bar{B}$) fields are large in the position sensing region of the chamber. To a first approximation the average position of a track is unaffected since the forces are symmetric about the track centre. However, these forces can significantly change the anode charge distribution. In a coordinate system in which x is along the wire, y is normal to the wire and z is parallel to the magnetic field, the electrons drift with velocity v_y toward the anode. A $\bar{V}\times\bar{B}$ force results which causes the electrons to drift at an angle α (the Lorentz angle) to the y direction where

$$\tan\alpha = \omega\tau \ . \tag{8}$$

Electrons drifting toward the anode wire will reach the wire with a displacement proportional to tan α.

Figure 3b illustrates the electron drift in the slot in the x-y plane as determined by Eq. (8). The

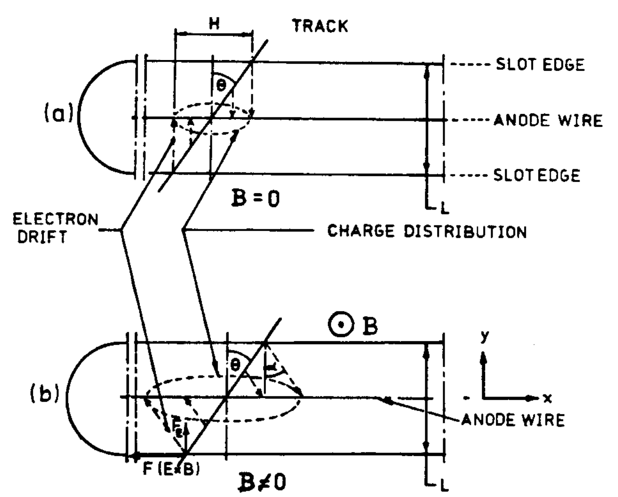

Fig. 3. Electron drift in the anode region. a) In the case of no magnetic field, the electrons drift in the y-direction and the charge is distributed along the anode in the dashed region. b) The magnetic field is out of the plane of the figure and the electrons drift under the Lorentz force at the angle α. The charge is spread along the anode in the dashed region. If θ =-α the charge spread neglecting diffusion is zero.

*Since the distributions approximate a normal distribution it is assumed that if the width is due to a number of independent contributions then the individual widths can be added in quadrature. The FWHM is taken to be 2.35 times the rms (root mean square) deviation.

actual electron path is not a straight line in the x-y plane since τ varies considerably during the drift, particularly in the region close to the wire. However, the data is adequately reproduced by assuming τ is constant and using an average value of tan α.

Including the additional term which accounts for the $\vec{E}\times\vec{B}$ angle α, the width of the distribution as a function of track angle is given by

$$W_3 = \frac{2.35L(\tan\theta - \tan\alpha)}{2\sqrt{3}} . \quad (9)$$

Variation of Total Width

The calculated cathode charge distribution has a FWHM which is the quadratic sum of the above components W_1, W_2 and W_3:

$$\phi^2 = W_1^2 + W_2^2 + W_3^2$$

$$= C_1^2 + \frac{C_2^2 z}{\cos^2\theta} + C_3^2(\tan\theta - \tan\alpha)^2 . \quad (10)$$

C1, the minimum width, includes the intrinsic width of the cathode charge distribution plus diffusion effects in the slot, electronic noise and other unknown components.

$$C_2 = 2.35\sqrt{\frac{2D(0)}{U(1+\omega^2\tau^2)}} \quad (11)$$

represents the effects due to diffusion in the drift region of the chamber and

$$C_3 = \frac{2.35\ L'}{2\sqrt{3}} \quad (12)$$

takes into account the crossing angle and $\vec{E}\times\vec{B}$ effects in the slot. Here L' is the effective slot width. From Eq. (10) it can be seen that the width is symmetric about θ=0 only when tanα is zero, i.e. B=0. In the case of B$\neq$0, the minimum width occurs at an angle θ_{min} which depends on both B and the drift distance z. By differentiation of Eq. (10) with respect to θ it is found that

$$\frac{1}{\tan\theta_{min}} = \frac{1}{\tan\alpha} + \frac{C_2^2 z}{C_3^2 \tan\alpha} . \quad (13)$$

The minimum width occurs at an angle θ_{min} which decreases as z increases.

Spatial Resolution

The spatial resolution depends on the precision with which the centroid of the charge distribution on the anode can be determined. For a point charge the resolution will depend on a number of poorly determined factors such as electronic noise, diffusion in the slot, fitting uncertainties and other factors. The parametrization of the resolution includes all these effects in a single parameter C_0.

As the track moves away from z=0 the effects of diffusion become important. When the crossing angle changes from the Lorentz angle the centroid of the charge distribution is affected by the charge distribution along the track. At atmospheric pressure the rms deviation of the centroid of the distribution is dominated by the clustering of the charge along the track. The FWHM of the resolution is[3]

$$\rho^2 = C_0^2 + \frac{C_2^2 z}{N_i \cos\theta} + \frac{C_3^2(\tan\theta - \tan\alpha)^2\ R\cos\theta}{N_i} \quad (14)$$

where R is the ratio of the second to first moment of the charge distribution deposited along the track. N_i is the number of electrons projected onto the normal to the slot direction. The second term is the contribution of diffusion to resolution and third term takes into account the crossing angle and clustering. R has been evaluated from the calculated charge distributions of Lapique and Puiz[4] to be R=7.5. The last term in Eq. (14) dominates the resolution at angles significantly different from α due to the large value of R.

Results

Width as a Function of Angle

Data from cosmic ray events that went through a single sector of the TPC were fitted to Eqs. (10) and (13) and the resultant parameters were extracted. The diffusion constant, $\omega\tau$ and α have been derived and the resolution compared with that predicted by Eq. (14). Magnetic fields of 0, 2.3, 4.1, 5.7 and 8.5 kG were used. The data have been divided into bins of constant drift length z, averaged over the angle of the track to the z-axis, and the width of the cathode charge distribution plotted against the angle at which the track crossed the wire, θ. A typical set of measurements is shown in Fig. 4. It displays the main features of the width variation described in the previous section. The most important feature is the asymmetric position of the minimum relative to θ=0 caused by the $\vec{E}\times\vec{B}$ effect in the slot. The minimum occurs close to the angle α at z= 3.5 cm and it moves towards θ=0 as z is increased, as predicted by Eq. (10).

Equation (10) also predicts that a plot of the width squared vs z at θ=0 will be a straight line. Figure 5 shows such plots for various magnetic fields, and from them the values of C2 for varying B were obtained. C2 is related to the diffusion constant D, and the mean time between collisions in the gas, τ, according to Eq. (11). Table I lists the observed values of C2, D, τ and $\omega\tau$ and the predicted value of $\omega\tau$, using the equation (in Gaussian units) taken from ref. 1:

$$\omega\tau = B^*U/(E^*c) \quad (15)$$

where c is the velocity of light. Figure 6 is a plot of $\omega\tau$ versus B and shows that the relation is linear, as expected since τ is independent of B.

According to Eq. (13) 1/tanθ_{min} is proportional to z, and has an intercept which is related to the angle α which describes the $\vec{E}\times\vec{B}$ effects near the anode wire. The angle θ_{min} was determined by fitting the data to Eq. (13) with z and B fixed. Figure 7 shows a plot of

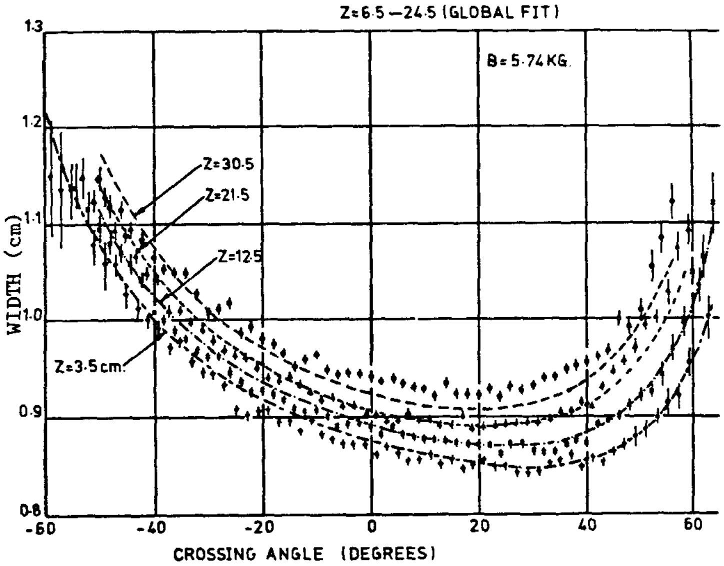

Fig. 4. The measured width of the pad distributions as a function of crossing angle for the case of B=5.74 kG. The four curves are for the drift distances shown and are averaged over a 3.0 cm interval. The curves are the result of fitting Eq. (10) to the data over drift distances from 6.5 to 27.5 cm. The χ^2 per degree of freedom of this fit was 1.3

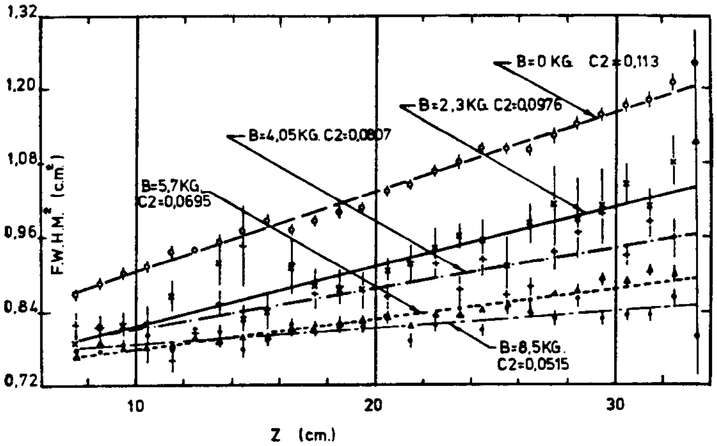

Fig. 5. The plots of $FWHM^2$ vs drift distance for the 5 magnetic fields studied. The slope is proportional to the diffusion constant and decreases with increasing magnetic field. The constant C_2 is proportional to the diffusion constant.

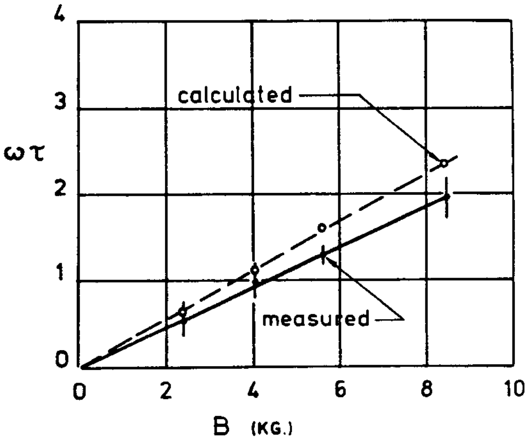

Fig. 6. Measured and calculated value of $\omega\tau$ vs magnetic field.

Table I.

B(Tesla)	C_2(mm)	$\omega\tau$	$\omega\tau$(Calc.)	τ(sec*10^{-11})	D(mm^2/sec)
0.00	0.356 ± 0.006	0	0	-	(8.0 ± 0.8)10^5
0.23	0.309 ± 0.025	0.61 ± 0.2	0.64	1.4 ± 0.5	(6.1 ± 1.4)10^5
0.41	0.255 ± 0.022	1.0 ± 0.2	1.13	1.4 ± 0.3	(4.1 ± 10.)10^5
0.57	0.220 ± 0.006	1.3 ± 0.1	1.61	1.3 ± 0.1	(3.1 ± 0.4)10^5
0.85	0.163 ± 0.016	1.9 ± 0.3	2.38	1.3 ± 0.2	(1.7 ± 0.5)10^5

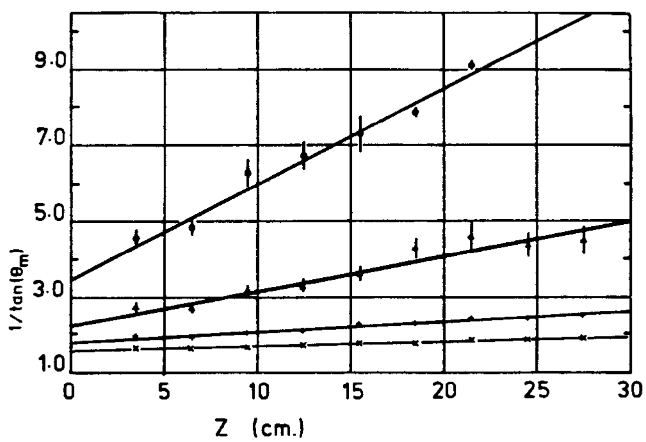

Fig. 7. Plots of 1/tan θ_{min} vs z. The solid lines are least squares fits of 1/tan θ_{min} vs z. The intercepts are equal to 1/tanα.

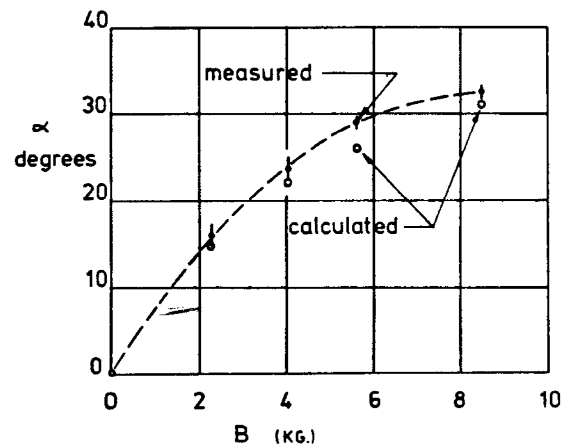

Fig. 8. The measured and calculated values of the Lorentz angle α in the anode slot as a function of magnetic field.

1/tan θ_{min} versus z, from which the angle α was determined. Figure 8 shows the measured and calculated values of α.

Resolution

Using the parameters determined above, the position resolution along the anode wire has been calculated using Eq. (14) for B=8.5 kG. The data has been plotted in Fig. 9 for short drift distances z ~ 3 cm. The lower solid line represents the calculated resolution. C_0 has been set equal to 180 μm, the value at the minimum. The upper curve is the calculated resolution for z=34 cm, the maximum drift distance.

The resolution deteriorates away from the minimum and is asymmetric. At B=8.5 kG, the diffusion has only a small effect on the resolution even for the longer drift distances as can be seen by the small increase in the widths represented by the upper curve in Fig. 9. The variation of resolution is strongly dependent on the value of R in the last term in Eq. (14) which results from the clustering of the primary ionization. The resolution may be improved by reducing R, reducing C_3 or increasing N_i. C_3 is proportional to the width of the track which is accepted and one may reduce this at the cost of reducing N_i. Increasing the pressure would reduce R and also increase N_i.

The asymmetry of the position resolution about θ=0 has consequences for the momentum resolution of charged particles traversing the chamber. Since the present system is designed to observe a limited ~70° arc of the trajectory for particles which fire both the inner and

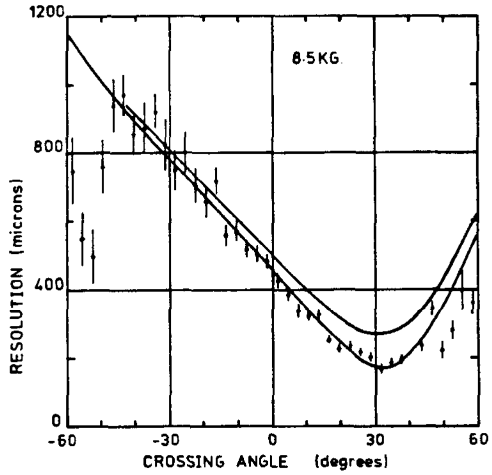

Fig. 9. The resolution as a function of crossing angle θ. The data are for 3.5 cm drift distance and B=8.5 kG. The curves are produced from Eq. (14). The lower (upper) curve uses z=3.5 cm (34 cm).

outer trigger scintillators, negative and positive particles tend to cross the anode wires at $\theta > 0°$ and $\theta < 0°$, respectively. For p=100 MeV/c and B=8.5 kG the average crossing angle is $\bar{\theta} \approx 30°$ for negatively charged particles and is $\bar{\theta} \approx -30°$ for positively charged ones. This results in considerably better position resolution and consequently is expected to result in better momentum resolution for negatively charged particles. Based on the results of this analysis the momentum resolution (FWHM) of the TPC expected for 100 MeV/c electrons is $\Delta P/P \sim 4\%$ and for 100 MeV/c positrons $\Delta P/P \sim 6\%$.

Conclusions

The position resolution of the TRIUMF TPC has been measured for Ar-CH_4 (80-20) at atmospheric pressure at electric field E=250 v/cm and with magnetic field B= 8.5 kG. A formulation has been worked out which describes the behavior of the resolution quantitatively. The factors contributing to the resolution involve diffusion, track-anode crossing angle, Lorentz forces and charge clustering of the initial ionization.

The resolution is determined by the precision with which the centroid of the charge distribution on the anode may be determined. The induced charge distribution on the cathode pads has been measured as a function of magnetic field. The diffusion constant, $\omega\tau$ in the drift region, and the Lorentz angle in the anode region have been determined and are in reasonable agreement with expectations.

It has been found that the minimum resolution at the Lorentz angle is $\sigma \sim 180$ µm. This rapidly deteriorates as the angle moves away from the Lorentz angle due to the large rms deviations of the centroid of the track charge distribution caused by the discrete nature of the primary ionization.

References

1. D. Nygren et al., SLAC PEP-4 proposal.
2. C.K. Hargrove et al., Physica Scripta 23, 668 (1981).
3. H. Mes et al., to be published.
4. F. Lapique and F. Puiz, Nucl. Instrum. and Methods 175, 297 (1980).